JOURNAL OF NATURAL REMEDIES
DOI: 10.18311/jnr/2025/49201
RESEARCH ARTICLE

An *In Silico* Pharmacophore-driven Virtual Screening and Molecular Docking for Identifying Potential AKT Inhibitors of Natural Origin

R. Sanjana, Sathiyapriya Palani, A. Varshini, Devakeerthana Manthrachalam, Venkatesan Saravanan, G. V. Anjana and Chagaleti Bharath Kumar*

Department of Pharmaceutical Chemistry, SRM college of Pharmacy, Faculty of Medicine and Health Sciences, SRMIST, Kattankulathur, Chennai - 603203, Tamil Nadu, India; bharathkumarchagaleti@gmail.com

Abstract

Background: Breast cancer accounts for 6.9% of cancer-related fatalities and 11.7% of new cases globally, making it the most often diagnosed cancer. Primarily seen in breast cancer is hyperactivation of the AKT/PI3K/mTOR pathway. Key signalling protein in this mechanism, AKT is essential for cell survival, proliferation, therapeutic resistance, and cancer progression. **Aim:** This study aims to identify potent phytochemical derivatives from the ZINC Natural derivatives database through virtual screening using known standard drugs. It integrates the pharmacophore features of selective compounds to screen a natural compound library, identifying potential anticancer agents. **Methods:** A ligand-based pharmacophore model was initially developed and validated by using known potent phytoconstituents such as Berberine, Lycorine, Noscapine, and Haemanthidine (IC_{50} < 20 µM). A validated model having four key features was used to screen the ZINC Natural derivatives database and identified 612 hits with essential AKT inhibitory features and further subjected to molecular docking studies. ADMET analysis and pharmacokinetic properties were assessed for the top lead compounds. **Results:** Molecular docking studies found ZINC 20412215 was the most potent AKT inhibitor, with a docking score of -8.36 kcal/mol, than the standard drug Capivasertib (-8.07 kcal/mol). It exhibits better aqueous solubility, high gastrointestinal absorption, and a lower likelihood of CYP2D6-mediated metabolic interference compared to Capivasertib. It is non-hepatotoxic and cytotoxic, with potential metabolic interactions of the molecules. **Conclusion:** These findings revealed that the compound ZINC 20412215 is a potential lead for AKT-targeted breast cancer therapy. Further experimental validation is required to advance its development as an effective anticancer agent.

Major Findings: The study identified novel AKT inhibitors from the ZINC natural compound library using pharmacophore modeling, docking, and ADMET analysis. Among them, ZINC 20412215 emerged as the most promising lead, combining strong binding affinity with favorable pharmacokinetic and toxicity profiles.

Keywords: AKT, Breast Cancer, Molecular Docking, Natural compounds, Pharmacophore Modelling

Abbreviations: ADME – Absorption, Distribution, Metabolism, and Excretion; AKT – Protein Kinase B; BC – Breast Cancer; HBA – Hydrogen Bond Acceptor; HBD – Hydrogen Bond Donor; HCPT – 10-Hydroxycamptothecin; HER-2 – Human Epidermal Growth Factor Receptor 2; IC50 – Half-Maximal Inhibitory Concentration; MOE – Molecular Operating Environment; PDB – Protein Data Bank; PD-1 – Programmed Cell Death Protein 1; PDL-1 – Programmed Death-Ligand 1; PI3K – Phosphoinositide 3-Kinase; PIK3CA – Phosphatidylinositol-4,5-Bisphosphate 3-Kinase Catalytic Subunit Alpha; PTEN – Phosphatase and Tensin Homolog; RMSD – Root Mean Square Deviation; TNBC – Triple-Negative Breast Cancer; TPSA – Topological Polar Surface Area

1. Introduction

Cancer remains a significant cause of global disease burden and mortality, with an estimated incidence of over 14 million new cases in recent years. Despite significant advancements in research, effective cancer treatment remains a challenge. Breast cancer accounts for 11.7% of newly diagnosed cancer cases and 6.9%

*Author for correspondence

Article Received on: 30.03.2025 Revised on: 29.09.2025 Accepted on: 05.12.2025

of cancer-associated deaths globally. The total cancer burden has increased, reaching approximately 18.1 million cases in 2018, highlighting the urgent need for additional therapies and interventions. In 2020, Breast Cancer (BC) was the most frequently diagnosed cancer in females, and coinciding with lung cancer in males[1]. According to the GLOBOCAN database, breast cancer is the leading malignancy among women, with an estimated 2.3 million new cases documented in recent years[2,3]. Projections indicate that by 2040, 40% rise, whereas deaths may increase by more than 50% to 1 million cases[4,5].

Breast cancer is classified into sub types like Luminal A, Luminal B, Human epidermal growth factor receptor 2-over expressing, and Triple-Negative Breast Cancer (TNBC) depending on hormone receptor status, cellular markers, and genetic mutations. The treatments are surgery, chemotherapy, radiation, hormonal therapy, targeted and immune-therapies. Aggressive TNBC is not responsive to hormonal and targeted treatments. Whereas recurrence and drug resistance remain the biggest hurdles, results in the identification of novel therapeutic agents[6-8].

Various synthetic analogues are available on the market for various diseases such as cancer treatment[9]. However, their associated side effects have shifted the focus toward natural compounds. Natural products exhibit effective cancer therapy through their structural diversity and unique biological properties[10]. Natural compounds are derived from plants, microbes, fermentation products, and marine organisms, demonstrating strong anticancer activity. Paclitaxel, a diterpene alkaloid derived from the Pacific yew plant, is one of the most well-known natural product-based drugs since its strong binding affinities to particular molecular targets help to cure breast, ovarian, and lung tumors. Another drug, 10-Hydroxycamptothecin (HCPT), a Camptothecin derivative, is recognised as one of the most effective anticancer compounds with its lower toxicity.

By altering important physiological processes, including angiogenesis, cell proliferation, differentiation, invasion, migration, and metastases, these natural chemicals have shown potential in lowering breast cancer mortality and improving patient outcomes. Given the rising burden of breast cancer and the limitations of current therapies, natural product-based treatments offer promising therapeutic opportunities to address this global health challenge[11]. For breast cancer therapy, about 60% of the drugs came from natural products. Phytochemicals exhibit excellent efficacy with less toxicity. These compounds mainly function as antioxidants, mitotic disruptors, and enzyme inhibitors.

Alkaloids are nitrogen-containing compounds obtained from various plants with varied therapeutic uses. These are mainly classified based on their origin (true, proto, and pseudo-alkaloids) and structure (*e.g.*, piperidine, isoquinoline, tropane, quinoline, purine, and steroidal alkaloids). Alkaloids are showing broad therapeutic action like anti-inflammatory, neuroprotective, antiviral, antimicrobial, and anticancer activities. Their ability to regulate key cellular functions makes them promising candidates for cancer treatment[12,13]. Certain phytochemicals, including flavonoids, alkaloids, and terpenoids, have demonstrated effective AKT inhibitory activity, promoting apoptosis and suppressing tumor growth in preclinical studies[14].

The PI3K-AKT pathway plays a significant role in breast cancer, with PIK3CA mutations accounting for 40% of ER+ cases. This pathway regulates cell proliferation and apoptosis, making it a promising drug target, especially in overcoming endocrine and anti-RTK resistance[15]. Additionally, phytochemicals exert their effects by directly binding to the AKT kinase domain, modulating upstream regulators such as PI3K and Phosphatase and Tensin homolog (PTEN), and enhancing downstream apoptotic signalling pathways[16,17]. By inhibiting AKT phosphorylation and activation, natural agents effectively restore normal cell cycle control and suppress tumour growth. Furthermore, natural AKT inhibitors have shown synergistic effects with standard chemotherapeutic drugs, helping to overcome drug resistance and enhance treatment efficacy[18,19]. Their ability to regulate multiple oncogenic pathways makes them ideal candidates for combination therapy in cancer treatment. AKT has three isoforms, AKT1, AKT2, and AKT3, that play key roles in controlling cell growth, survival, and drug response which is shown in Figure 1[20,21]. MK-2206, an allosteric AKT inhibitor, is sensitive in PIK3CA-mutant and PTEN-deficient breast cancer but is limited in efficacy[22]. Combination therapies, including

MK-2206 with lapatinib or anastrozole, are confronted with toxicity issues. AKT inhibitors AZD5363 and GDC-0068 are promising in PTEN-altered tumors. Combining Receptor tyrosine kinases (RTK and MEK inhibitors may improve efficacy but enhance chemotherapy side effects[23,24].

Computer-aided drug design plays a vital role in the drug discovery cycle through the identification of effective AKT-targeting compounds using structure-based and ligand-based strategies[25-28]. Pharmacophore modelling helps one to identify important chemical characteristics required for AKT inhibition, including π-ring interactions, hydrogen bond donors or acceptors, and hydrophobic or aromatic hydrophobic centers. After that, docking studies were done to forecast the molecular interaction of the hits with the AKT; the produced hits were then subjected to ADMET analysis to evaluate their pharmacokinetic characteristics and toxicity risk. These *in silico* approaches facilitate the identification of highly specific, drug-like lead candidates[29]. The present study leverages these methodologies to provide a systematic and rational framework for selecting and optimising the key molecular features of natural compounds as potential AKT inhibitors[30].

2. Materials and Methods

2.1 Selection of the Dataset

A literature review on the anti-breast cancer potential of natural compounds was carried out with a particular focus on their AKT inhibitory potential. Phytochemicals which were reported to demonstrate high inhibition levels against AKT (IC_{50}≤ 20 or lower) were selected to undergo further examination. On this basis, four strong compounds were obtained. Berberine, Lycorine, Noscapine, and Haemanthidine illustrated in Figure 2 were found, and chemical structures were obtained in the PubChem database with IC_{50} = 15.47 µM, 7.76 µM, 16 µM, and 2.7 µM, respectively. These were later used to develop the pharmacophore model[31-33].

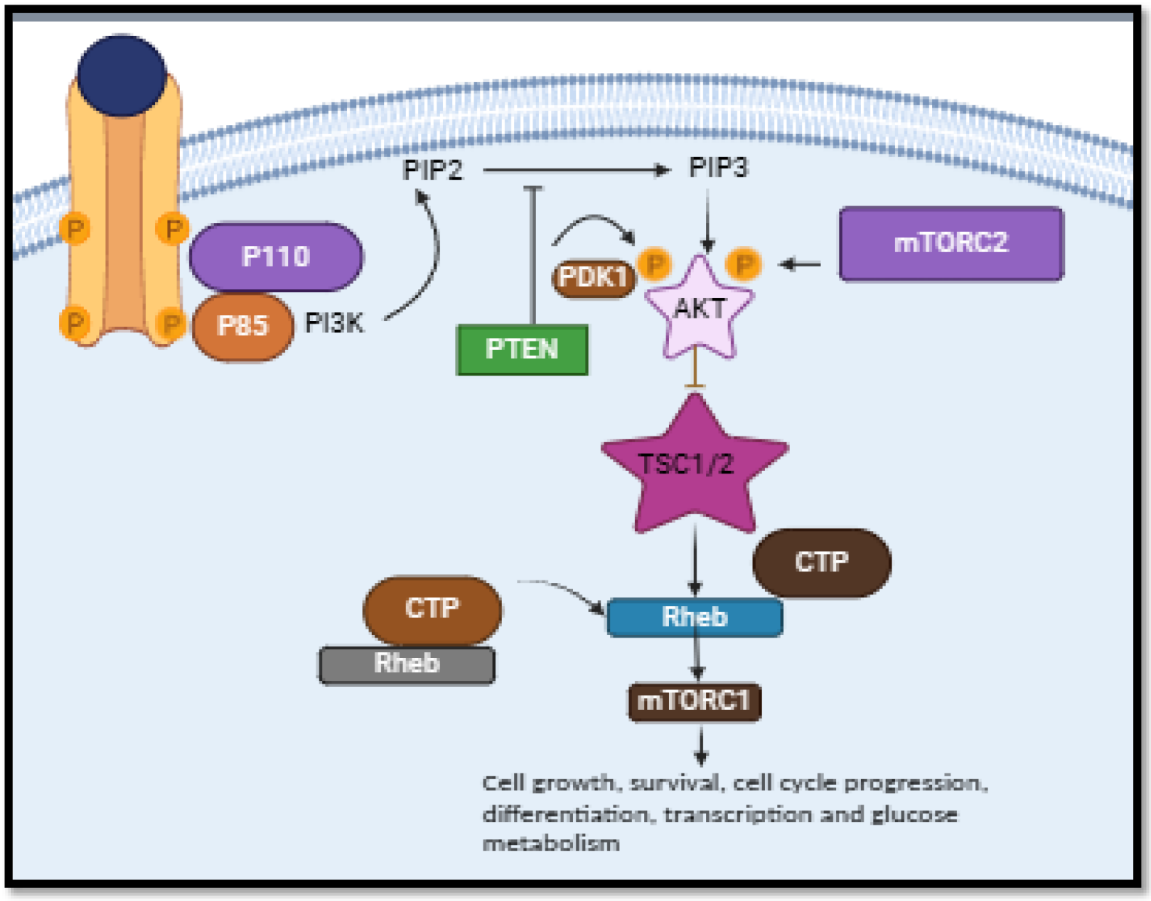


Figure 1. AKT signaling pathway.

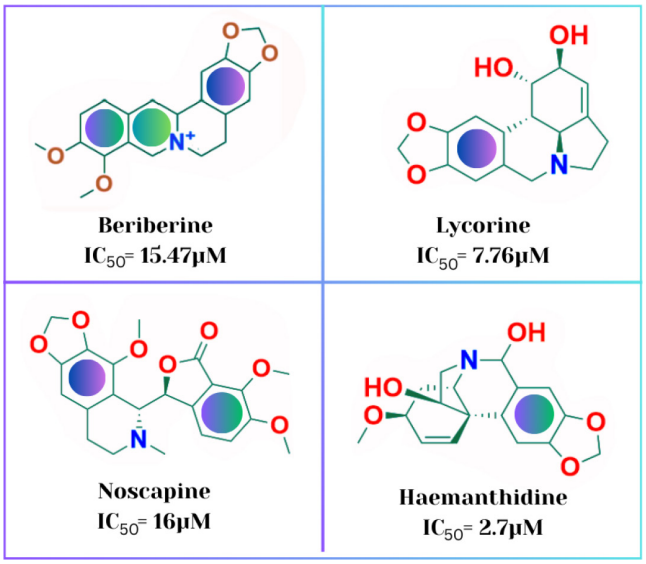


Figure 2. Potent natural constituents inhibiting AKT employed to develop a pharmacophore model.

2.1 Generation of Pharmacophore Model

MOE® was used to energy-minimise the molecular structures of the chosen natural compounds with the Amber 10: EHT force field and the lowest-energy conformers were oriented with the Flexible Alignment tool. The Pharmacophore Query Editor was used to create a consensus pharmacophore model at a tolerance of 1.2 Å, and the best-aligned pharmacophore model with the lowest S value was selected[34]. The model exposed the major pharmacophoric properties, including Pi-ring Normal (PiN), Hydrophobic centre (Hyd), Aromatic Hydrophobic centres (AroHyd), Hydrogen Bond Acceptor (Acc), and Hydrogen Bond Donor (Don), which match the crucial binding elements of AKT active sites and, therefore, offer a rational model in the discovery of the inhibitor. This model was then optimised, and pharmacophore-based virtual screening of the ZINC database was done to identify potential hits[35].

2.2 Pharmacophore Validation

The validation studies were conducted to assess the reliability of the developed pharmacophore model and its effectiveness in distinguishing active compounds from decoys. To perform the validation, a known dataset of decoy compounds was retrieved using the DUD-E database. The pharmacophore model was assessed using the standards listed below.

Sensitivity = True Positive / True Positive + False Negative

Specificity = True Positive / True Positive + False Negative

Non-Error Rate = Sensitivity + Specificity / 2

The validated pharmacophoric hypothesis was employed to search the ZINC natural derivative database in order to identify structurally similar compounds exhibiting comparable pharmacophoric features[36].

2.3 Molecular Docking

Pharmacophore-based hits were further analysed using molecular docking in MOE® 2022, with AKT (PDB ID: 8Q61) as the target protein. The selected crystal structure, relevant to breast cancer, had a resolution of 2.32 Å, an R-value free of 0.263, and no Ramachandran outliers. Protein preparation involved removing water molecules, cofactors, and heteroatoms, followed by protonation to optimise hydrogen bonding and energy minimization. The active site was defined using the Site Finder module which identified 398 residues as the most potent active site. A total of 612 natural derivative hits from the ZINC database were geometry-optimised with the Amber10: EHT force field and docked into the AKT binding site using the Dock module. The triangle matcher algorithm generated 5 conformations per ligand, which were scored with the London dG scoring function, and the top-ranked poses were selected. Ligand-protein interactions were visualized in both 2D and 3D formats, compared with the co-crystallized ligand, and further analysed through hydrogen bond interactions and binding free energy calculations to evaluate binding affinity[37].

2.4 Physicochemical Properties

The pharmacological effectiveness of drugs is largely determined by their physicochemical properties, which influence their behaviour in biological systems. Critical parameters such as Log P, molecular weight, the number of hydrogen bond donors and acceptors, and Topological Polar Surface Area (TPSA) are key determinants of a compound's pharmacokinetic profile. These properties were calculated using Molinspiration, a web-based cheminformatics tool. According to Lipinski's rule of five, compounds with Log P ≤ 5, molecular weight ≤ 500 Da, hydrogen bond donors ≤

5, and hydrogen bond acceptors ≤ 10 are more likely to exhibit favourable oral bioavailability[38]. Deviations from these thresholds may impair absorption or reduce bioavailability. The calculated parameters were therefore used to assess the drug-likeness and potential oral absorption of the selected compounds.

2.5 Pharmacokinetic Properties

ADME properties significantly influence the biopharmaceutical characteristics of drugs, which directly impact their efficacy, safety, and overall pharmacokinetic profile[39,40]. Analysing these characteristics helps optimize drug design by identifying structural-property relationships, addressing potential pharmacokinetic or toxicity concerns, and refining bioassay interpretation. Compounds with optimal pharmacokinetic profiles tend to exhibit improved potency and safety in therapeutic applications. The Swiss ADME, a web-based tool, was utilized to predict the ADME properties of the screened compounds[41].

2.7 Toxicity

In silico toxicity prediction is a valuable tool for uncovering potential risks while reducing the reliance on extensive *in vitro* and *in vivo* testing. This computational method accelerates drug discovery and guides in identifying compounds with a desirable toxicological profile. Advances in predictive modelling have significantly enhanced the capacity to evaluate the toxicological risk of new chemical entities, thereby contributing to the development of safer pharmaceuticals[42]. The ProTox-III web server was employed to evaluate the toxicological profiles of the hit compounds. Multiple toxicological endpoints such as hepatotoxicity, carcinogenicity, immunotoxicity, mutagenicity, and cytotoxicity were evaluated to ascertain the safety profiles of the selected hit compounds[43-45].

3. Results

3.1 Pharmacophore Modeling

Pharmacophore modelling was employed to identify key molecular features essential for AKT inhibition. A structurally diverse set of natural compounds, known for their AKT inhibitory potential with IC_{50} values below 20 µM, was selected. The compounds were optimised to their lowest-energy conformers using the Amber 10: EHT force field, followed by alignment using MOE's Flexible Alignment Tool. A consensus pharmacophore model was created with a threshold of 80% and a tolerance limit of 1.2 Å,

Table 1. Features of pharmacophore model of selected molecules

S. No.	Features	Colour
F1	Hyd	Green
F2	Aro|Hyd	Orange
F3	Acc	Red
F4	Cat|Acc	Blue

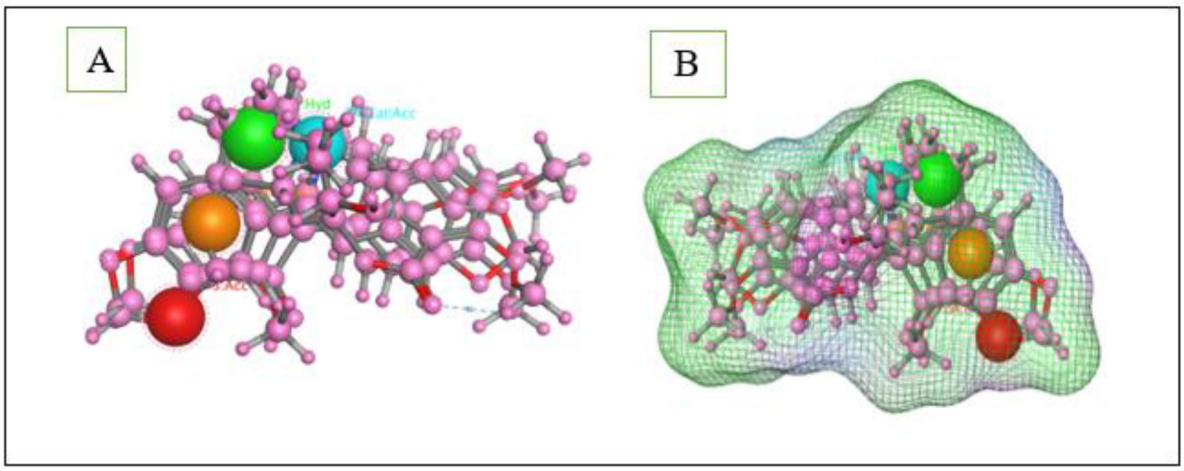


Figure 3. **(A).** Best alignment of selected natural constituents; **(B).** Selected pharmacophore features identified for the development of AKT inhibitor.

incorporating four essential features: A hydrophobic centre (Hyd), an Aromatic Hydrophobic region (Aro/Hyd), a hydrogen bond acceptor (Acc), and a positively charged or acceptor feature (Cat/Acc) as depicted in Table 1. Figure 3 (A) and (B) represent the best alignment of selected natural compounds andcommon pharmacophore features of AKT inhibitors. This model was subsequently used to screen a chemical database for potential AKT inhibitors.

3.2 Pharmacophore Validation

For validation, the pharmacophore model was screened against a dataset of 184 known AKT inhibitors and 6692 decoys. Despite comprising only four phytoconstituents, the training set was selected for their reported low IC_{50} values, ensuring both potency and structural diversity. The model successfully identified 163 actives and 3181 decoys, achieving a sensitivity of 0.88, demonstrating that the model accurately identified 88% of the active compounds. The specificity and non-error rate were both above 50%, reflecting moderate accuracy in excluding non-actives. The IC_{50} values of the training compounds, along with strong sensitivity and consistent recognition of actives, confirm that the pharmacophore model is robust and suitable for virtual screening of AKT inhibitors.

3.3 Virtual Screening in ZINC Natural Derivatives Database

Following successful validation, the pharmacophore model was applied to screen the ZINC natural compound derivatives library, aiming to identify novel AKT inhibitors. The screening process incorporated parameters such as an RMSD threshold of 0.3, molecular weight restricted to 500 Da or lower, and a limit of 3 rotatable bonds to ensure drug-likeness and bioavailability. This screening process resulted in the identification of 612 hit compounds that matched the essential pharmacophoric features required for AKT inhibition.

3.4 Molecular Docking

Molecular docking studies were carried out to assess the binding affinity and interaction profile of the virtual screened compoundswith AKT (PDB ID: 8Q61), as represented in Figure 4. The docking scores of the ZINC molecules summarized in Table 2 ranged between -8.74 and -7.73 kcal/mol, which are comparable to the standard inhibitor capivasertib (-8.07 kcal/mol). The reference natural compounds berberine (-6.86 kcal/mol), lycorine (-6.02 kcal/mol), noscapine (-7.32 kcal/mol), and haemanthidine (-5.82 kcal/mol) exhibited weaker binding affinities, suggesting that the ZINC natural compounds have higher potential to stabilize the kinase domain of AKT.

Capivasertib, used as the standard, showed strong binding through hydrogen bonds with Val187 and Ile189 (backbone donors) and hydrophobic interactions with Ala190 and Lys111. This profile reflects its known role as an AKT inhibitor. The ZINC compounds also displayed important binding interactions. Several ligands, such as ZINC 32109687, ZINC 20412215, ZINC 20412303, ZINC 70674573, ZINC 18062615, ZINC 20111621, ZINC 20112249, and ZINC 20111604, engaged residues including Trp80, Thr82, Leu212, Asp275, and Asp293, highlighting their ability to exploit diverse active binding sites within the kinase pocket.

Among these, ZINC 32109687 (–8.74 kcal/mol) demonstrated the highest affinity, forming a stabilizing aromatic interaction with Trp80, which indicates a strong π–π stacking contribution. It is also involved in metal ion contact with Asp293 residue. ZINC 20412215 (-8.36 kcal/mol) formed hydrogen bonds with Gln79 and metal ion contact with Arg274, while ZINC 20412303 (-8.04 kcal/mol) showed favourable interaction with Ttrp80 through Arene-arene contact and with Asp293 with Asp293 by metal ion contact. Compounds such as ZINC 70674573 and ZINC 18062615 further interact with Leu212 and Asp275 *via* hydrophobic and ionic contacts, contributing to stable binding. ZINC 20111621 and ZINC 20111604 also revealed consistent interactions with Asp293 and Trp80, indicating an interaction among the potent hits.

By comparison, the natural product references showed inferior binding. Berberine (-6.86 kcal/mol) formed only limited interactions with Asp275 and Thr82, while lycorine (-6.02 kcal/mol) interacted with Asp275, Asp293, and Gly295, but lacked strong hydrophobic anchoring. Noscapine (-7.32 kcal/mol) exhibited moderate binding *via* Trp80 (arene-H interaction), and haemanthidine (-5.82 kcal/mol) displayed the weakest affinity, interacting with Glu17 and Gln79.

Overall, the ZINC compounds particularly ZINC 32109687, ZINC 20412215, and ZINC 20412303, exhibited potential binding affinity and interaction compared to both the natural references and the standard capivasertib. Their ability to engage key residues such as Trp80, Thr82, Leu212, and Asp293 suggests they may serve as promising scaffolds for the design of novel AKT inhibitors. The 2D and 3D structures of the top 10 compounds are shown in Figures 5 and 6.

3.5 Physicochemical Properties

The physicochemical characteristics of the selected hits were analysed to assess their potential as drug candidates, focusing on molecular weight, lipophilicity (Log P), Topological Polar Surface Area (TPSA), Hydrogen Bond Acceptors (HBA), Hydrogen Bond Donors (HBD), and the number of Rotatable bonds (nRb) listed below in Table 3. The molecular weights of the hit compounds varies between 352.44 Da (ZINC 18062615) to 506.65 Da (ZINC 70674573), with most falling within the acceptable range for oral bioavailability as per Lipinski's Rule of Five, except for ZINC 20412303 and ZINC 70674573, which slightly exceed the 500 Da threshold. Log P values vary significantly, with compounds like ZINC 03850479 (4.78) being highly lipophilic, while others, such as ZINC 20412303 (-2.76) and ZINC 20412215 (-2.69), are more hydrophilic. The TPSA values range from 48.84 Å² (ZINC 20111604) to 118.07 Å² (ZINC 20412303), suggesting variations in membrane permeability and solubility. The number of HBA and HBD influences hydrogen bonding capacity, with compounds such as ZINC 01710113 having the highest HBA (7) and ZINC 18062615 lacking any hydrogen bond donors. Additionally, the number of Rotatable bonds (nRb) varies between 2 (ZINC 70674573 and ZINC 20112249) and 6 (ZINC 32109687), which can impact molecular flexibility and bioavailability. Except ZINC 20412303 and ZINC 70674573, all other compounds comply with the Lipinski rule and possess good oral bioavailability.

3.6 ADME Analysis

The pharmacokinetic properties of the top ten screened compounds and the reference drug Capivasertib are summarized in Table 4. Gastrointestinal (GI)

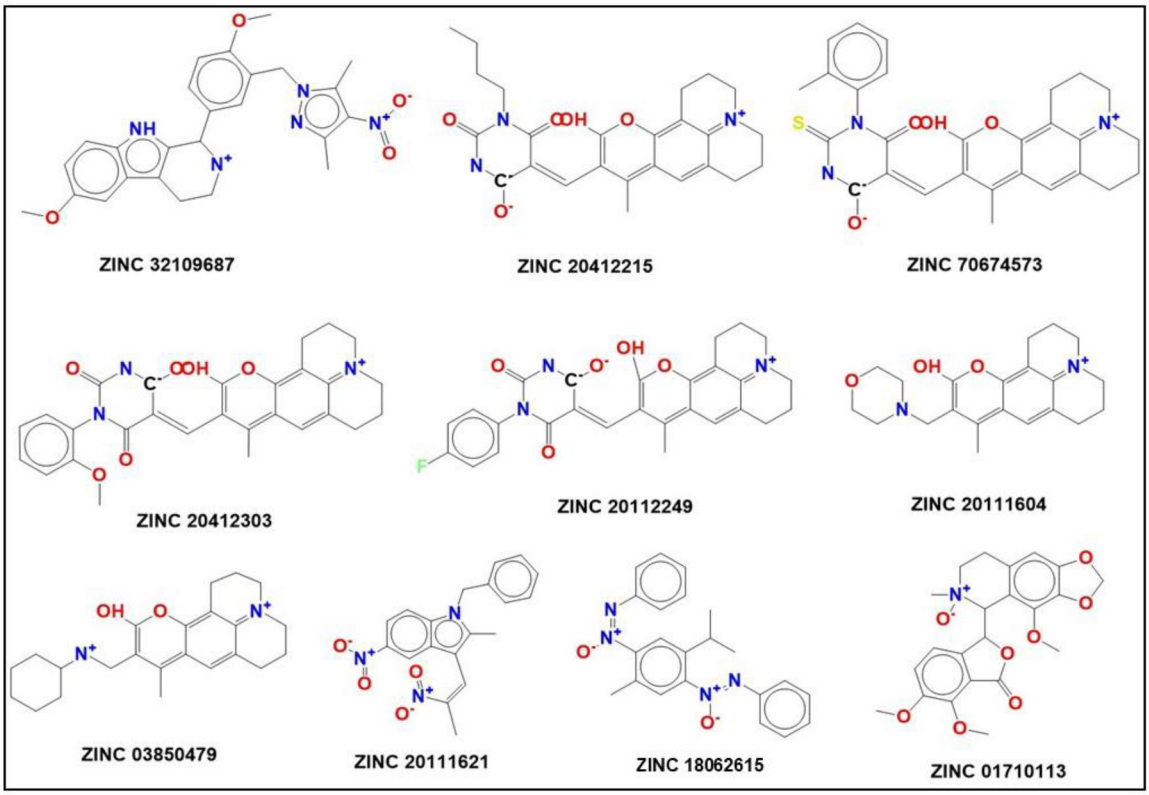


Figure 4. Top 10 compounds obtained from the screening of ZINC natural compounds database.

Table 2. Docking score and binding interactions of the top 10 screened compounds

ZINC IDs	Dock Score (K.cal/mol)	Hydrogen Interaction	Hydrophobic Interaction
ZINC 32109687	-8.74	-	Trp 80 (Arene arene), Asp293 (Metal ion contact)
ZINC 20412215	-8.36	Gln 79 (Side chain acceptor)	Arg274 (Metal ion contact)
ZINC 20412303	-8.04	-	Asp293 (Metal ion contact), Trp80 (Arene-arene)
ZINC 70674573	-8.03	-	Leu 212, Thr 82(Arene H), Asp 275 (Ion contact),
ZINC 18062615	-7.99	Gln 79 (Side chain acceptor)	Trp 80 (Arene arene)
ZINC 20111621	-7.96	Asp 293 (Side chain donor)	Trp 80 (Arene H)
ZINC 03850479	-7.88	-	Trp 80 (Arene H)
ZINC 20112249	-7.88	Thr 82 (Arene H, Side chain donor)	Arg274 (Metal ion contact)
ZINC 01710113	-7.73	-	Leu 212 (Arene H), Trp 80 (Arene H)
ZINC 20111604	-7.57	Asp 293 (Side chain donor)	Trp 80 (Arene H)
Standard (Capivasertib)	-8.07	Val187, Ile189 (Backbone donor)	Ala190, Lys111 (Arene H)
Beriberine	-6.86	Asp275 (side chain donor)	Thr82 (Arene-H)
Lycorine	-6.02	Asp275, Asp293 (side chain donor), Gly295 (back bone acceptor)	-
Noscapine	-7.32	-	Trp80 (Arene-H)
Haemanthidine	-5.82	Glu17 (Side chain donor), Gln79 (Side chain acceptor)	-

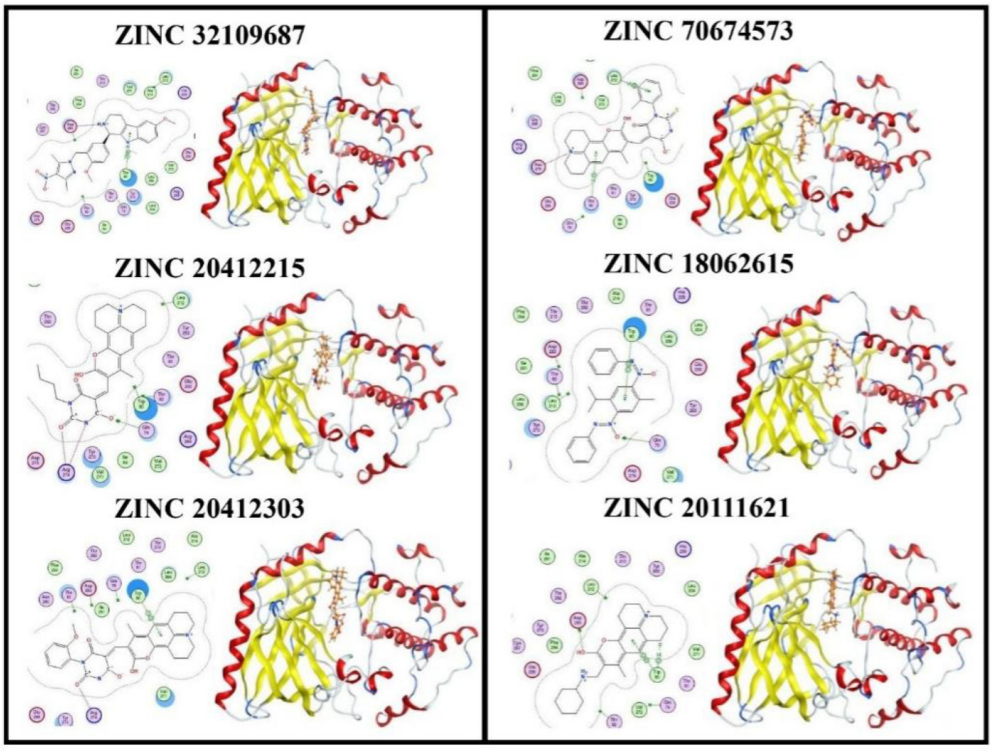


Figure 5. 2D and 3D molecular interaction visualisations generated for the top three ranked compounds, alongside the standard Capivasertib.

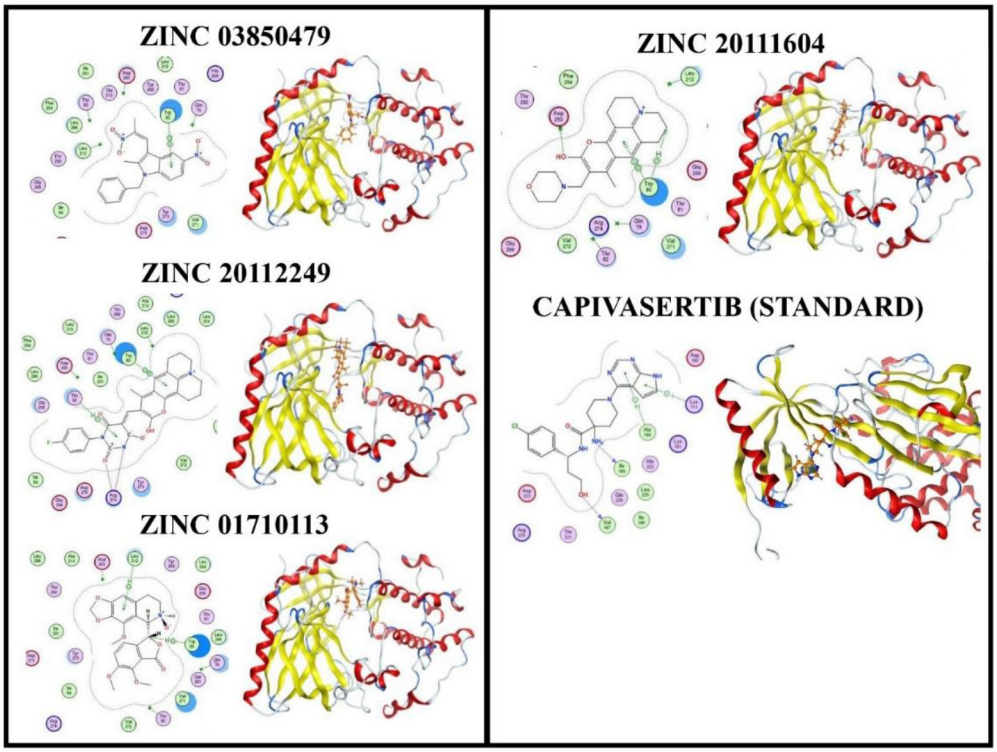


Figure 6. Visual representations of molecular interactions in both 2D and 3D formats for the other highest-ranking compounds and the standard.

Table 3. Physico-chemical properties of the top 10 docked compounds

ZINC IDs	Molecular Weight (g/mol)	logP	TPSA Å	HBA	HBD	nRb	No. of Violations
ZINC 32109687	480.67	-0.33	108.19	4	2	6	0
ZINC 20412215	450.51	-2.69	108.84	6	2	4	0
ZINC 20412303	506.58	-2.76	118.07	7	2	3	0
ZINC 70674573	506.65	-1.44	91.77	6	2	2	0
ZINC 18062615	352.44	-3.51	96.57	2	0	5	0
ZINC 20111621	368.52	-1.57	52.98	2	2	3	0
ZINC 03850479	365.37	4.78	94.89	7	0	5	0
ZINC 20112249	494.54	-2.91	108.84	6	2	2	0
ZINC 01710113	441.52	-0.80	89.55	7	0	4	0
ZINC 20111604	355.46	-0.57	48.84	5	1	2	0
Capivasertib	428.92	2.49	120.16	5	4	7	0

absorption, Blood-Brain Barrier (BBB) permeability, P-glycoprotein (P-gp) substrate status, Cytochrome P450 (CYP) inhibition, and skin permeation (Log Kp) were evaluated to assess the drug-likeness and potential pharmacokinetic behaviour of these compounds. Most compounds, including ZINC 20412215, exhibited high predicted gastrointestinal absorption, indicating strong potential for oral bioavailability. None of the compounds were predicted to cross the blood-brain barrier except ZINC 20111621, which is advantageous for targeted systemic therapy by minimising potential central nervous system side effects. ZINC 20412215, along with most other compounds, was identified as a P-glycoprotein (P-gp) substrate, indicating efficient efflux-mediated transport for controlled systemic exposure, whereas ZINC 03850479 did not exhibit P-gp

substrate activity, highlighting variability among the screened compounds. Several compounds, such as ZINC 20412215, ZINC 20412303, ZINC 20112249, ZINC 01710113, and ZINC 20111604, showed no inhibition across all major isoforms, suggesting a lower risk of metabolic drug-drug interactions. Skin permeation (Log Kp) values ranged from -4.43 to -8.71 cm/s, with more negative values reflecting lower permeability, which generally reduces the risk of dermal exposure-related toxicity. While several compounds demonstrated favourable pharmacokinetic characteristics, ZINC 20412215 combines high gastrointestinal absorption, absence of BBB permeability, non-inhibition of all major CYP enzymes, and low skin permeation, making it a particularly promising candidate for further development.

3.7 Toxicity Studies

The predicted toxicity profiles of the screened compounds, including hepatotoxicity, carcinogenicity, immunotoxicity, mutagenicity, and cytotoxicity, are summarized in Table 5. These parameters provide insights into the potential safety and biocompatibility of the compounds. Hepatotoxicity of the compounds, including ZINC 20412215, ZINC 20412303, ZINC 70674573, ZINC 20111621, ZINC 20112249, ZINC 20111604, and Capivasertib, was predicted as inactive with probabilities ranging from 0.53 to 0.79. These results suggest a low occurrence of liver-related adverse effects, indicating favourable hepatic safety. Carcinogenicity was predicted as inactive for ZINC20412215, ZINC20412303, ZINC70674573, ZINC20111621, ZINC20112249, ZINC20111604, and Capivasertib, with probabilities ranging from 0.51 to 0.55. The potential of a compound to affect the immune system was predicted as inactive for most compounds, including ZINC20412215, ZINC70674573, ZINC1802615, ZINC20111621, ZINC03850479, ZINC20112249, ZINC20111604, and Capivasertib, with probabilities ranging from 0.57 to 0.93. This indicates that these compounds are unlikely to compromise immune function. Only ZINC32109687 and ZINC01710113 were predicted as active with probabilities 0.69 and 0.98, respectively. Mutagenicity was inactive for the majority of compounds, including ZINC20412215, ZINC20412303, ZINC70674573, ZINC20112249,

Table 4. ADME properties of the top 10 docked compounds

ZINC IDs	GI Absorption	BBB Permeant	P-gp Substrate	CYP1A2 Inhibitor	CYP2C19 Inhibitor	CYP2C9 Inhibitor	CYP2D6 Inhibitor	CYP3A4 Inhibitor	Log K_p (Skin Permeation)
ZINC 32109687	High	No	Yes	No	Yes	Yes	No	Yes	-6.51 cm/s
ZINC 20412215	High	No	Yes	No	No	No	No	No	-8.59 cm/s
ZINC 20412303	High	No	Yes	No	No	No	No	No	-8.71 cm/s
ZINC 70674573	High	No	Yes	No	No	Yes	No	No	-8.00 cm/s
ZINC 18062615	Low	No	Yes	No	Yes	Yes	No	No	-4.43cm/s
ZINC 20111621	High	Yes	Yes	No	No	No	No	No	-7.09 cm/s
ZINC 03850479	High	No	No	No	Yes	Yes	No	Yes	-5.28 cm/s
ZINC 20112249	High	No	Yes	No	No	No	No	No	-8.54 cm/s
ZINC 01710113	High	No	Yes	No	No	No	No	No	-7.33cm/s
ZINC 20111604	High	No	Yes	No	No	No	No	No	-8.25cm/s
Capivasertib	High	No	Yes	No	No	No	Yes	Yes	-7.71cm/s

Table 5. Toxicity results of the top 10 docked compounds

Zinc IDs	Hepatotoxicity		Carcinogenicity		Immunotoxicity		Mutagenicity		Cytotoxicity	
	Prediction	Probability	Prediction	Probability	Prediction	Probability	Prediction	Probability	Prediction	Probability
ZINC 32109687	Inactive	0.60	Active	0.58	Active	0.69	Active	0.81	Inactive	0.59
ZINC 20412215	Inactive	0.65	Inactive	0.51	Inactive	0.62	Inactive	0.63	Inactive	0.63
ZINC 20412303	Inactive	0.59	Inactive	0.52	Active	0.78	Inactive	0.57	Inactive	0.59
ZINC 70674573	Inactive	0.54	Inactive	0.54	Inactive	0.90	Inactive	0.60	Inactive	0.61
ZINC 18062615	Active	0.50	Active	0.81	Inactive	0.97	Active	0.56	Inactive	0.77
ZINC 20111621	Inactive	0.74	Inactive	0.52	Inactive	0.83	Active	0.51	Inactive	0.54
ZINC 03850479	Inactive	0.61	Active	0.58	Inactive	0.62	Active	0.83	Inactive	0.51
ZINC 20112249	Inactive	0.53	Inactive	0.54	Inactive	0.73	Inactive	0.54	Inactive	0.68
ZINC 01710113	Inactive	0.67	Active	0.55	Active	0.98	Inactive	0.59	Inactive	0.63
ZINC 20111604	Inactive	0.79	Inactive	0.52	Inactive	0.93	Inactive	0.61	Inactive	0.53
Capivasertib	Inactive	0.69	Inactive	0.55	Inactive	0.97	Inactive	0.59	Inactive	0.74

ZINC20111604, and Capivasertib, with probabilities ranging from 0.53 to 0.61. The cytotoxicity was inactive for almost all compounds, including ZINC32109687, ZINC20412215, ZINC20412303, ZINC70674573, ZINC1802615, ZINC20111621, ZINC03850479, ZINC20112249, ZINC01710113, ZINC20111604, and Capivasertib, with probabilities mostly above 0.50. This indicates that the screened compounds are expected to exhibit minimal non-specific cytotoxicity, supporting their safety for further therapeutic development. This overall toxicity result suggests a favourable safety profile and minimal risk of adverse effects for the entire set of compounds.

4. Discussion

The PI3K/AKT/mTOR pathway plays a crucial role in breast cancer development, survival of cells, and resistance to drugs. A mutation in PIK3CA can disturb this pathway, leading to cancer by increasing AKT signalling. Premalignant and aggressive forms of breast cancer, such as invasive breast cancer (38%), and Ductal Carcinoma *In Situ* (DCIS) (33%), have AKT more expressed. Additionally, 40% of tumours in the breast have elevated AKT activity due to phosphorylation at Ser473, is to promote breast cancer growth and metastasis. Decreasing the expression of AKT inhibits cellular aggression, proliferation, and spreading of breast cancer. Thus, targeting this pathway is a viable therapeutic option in the treatment of breast cancer.

The pharmacophore model generated provides valuable information about the molecular characteristics needed for AKT inhibition. With a structurally diverse collection of natural compounds with IC_{50} values less than 20 µM, and optimised conformations of compounds ensured precise alignment, enhancing model validity. The pharmacophore model was constructed to recognise important features required for AKT inhibition in breast cancer. The pharmacophore model, having 4 features, a Hydrophobic centre (Hyd), an Aromatic Hydrophobic region (Aro/Hyd), a hydrogen bond acceptor (Acc), and a positively charged or acceptor feature (Cat/Acc) was selected. The model was 88% sensitive, with good capability to recognize true inhibitors, thus lowering the chances of false negatives. A specificity of more than 50% shows that it has a fair capability of distinguishing between active and inactive compounds. The model highlights a feature necessary for the best fit within the AKT binding site. Hydrophobic interactions are essential for anchoring the drug in the active site, as AKT has hydrophobic pockets that accommodatethe nonpolar part of ligands. Electrostatic and hydrogen bonding interactions also increase ligand specificity and binding affinity with the target.

The validated pharmacophore model was virtually screened in the ZINC natural compound derivative library to identify potential AKT inhibitors. Consequently, 612 natural compound derivatives were identified based on the significant pharmacophoric

features crucial for AKT inhibition. These compounds were progressed for further molecular docking and *in-silico* screening for targeting AKT.

Among the screened compounds, ZINC32109687 and ZINC20412215 exhibited the highest docking scores of -8.74 kcal/mol and 8.36kcal/mol, demonstrating a favourable orientation within the AKT binding site and forming key interactions with residues such as Asp293, Trp80 through arene-arene interactions and Gln 79. In comparison, Capivasertib (standard drug) showed a docking score of -8.07 kcal/mol with interactions involving Val187, Ile189, Ala190, and Lys111. The stronger binding affinity of ZINC20412215 and ZINC32109687 suggests its superior potential as AKT inhibitors. The top ten compounds based on docking scores were further evaluated for drug-likeness using Lipinski's rule and comprehensive toxicity profiling. ZINC20412215 emerged as the most promising lead, exhibiting favourable physicochemical properties compared to Capivasertib. Its pharmacokinetic profile is also advantageous, with high predicted gastrointestinal absorption suggesting improved oral bioavailability. Toxicity analysis revealed that all five toxicity parameters, hepatotoxicity, carcinogenicity, immunotoxicity, mutagenicity, and cytotoxicity, were predicted as inactive.

While ZINC 32109687 displayed the most favourable docking score (-8.74 kcal/mol) and strong stabilizing interaction with Trp80, its predicted toxicity profile raised significant concerns. The compound was flagged as "active" for carcinogenicity, immunotoxicity, and mutagenicity, which reduces its suitability for advancement despite its potency. This apparent contradiction between binding affinity and safety highlights the need to balance efficacy with drug-likeness and toxicity considerations. Structural optimization strategies, such as bioisosteric replacement of the aromatic moiety responsible for genotoxic alerts, could be explored to reduce its liabilities. However, such modifications would require extensive computational and experimental validation. Given these limitations, ZINC 20412215 emerges as a more viable candidate. Although it's docking score (-8.36 kcal/mol) was slightly lower than ZINC 32109687, it still showed strong binding through a hydrogen bond with Gln79 and favourable orientation within the ATP-binding pocket. Its ADMET profile did not reveal toxicity alerts, supporting its potential as a safer lead compound. Thus, in the present study, ZINC 20412215 has been prioritized as the most promising inhibitor due to its balanced combination of potent AKT binding and acceptable safety predictions.

5. Future Scope

The present study has certain limitations that need to be acknowledged. Primarily, the research relies on *in silico* pharmacophore modelling, virtual screening, and molecular docking without experimental *in vitro* or *in vivo* validation, which limits confirmation of the predicted biological activity and safety of the identified compounds. The pharmacokinetic and toxicity predictions, while useful, are computational and may not fully capture complexities in biological systems. Literature supports the utility of heterocyclic scaffolds as potential anticancer, reinforcing the importance of exploring diverse heterocycles that might cause pharmacokinetic and toxicity effects in later stages[46,47]. However, the screening was confined to a specific natural compound database, potentially overlooking other potent inhibitors outside this dataset. The molecular docking methodology, though robust, does not account for dynamic protein flexibility and full cellular context, which could influence binding efficacy and drug behaviour. Despite these limitations, the study lays a strong foundation for future research by identifying promising lead compounds with favourable binding affinity and pharmacokinetic properties targeting AKT in breast cancer. Experimental validation through biochemical assays and clinical investigations should follow to confirm efficacy and safety. Moreover, expanding the screening library and integrating molecular dynamics simulations can enhance the predictive power of this approach, ultimately supporting the discovery and development of novel, natural product-based anti-cancer therapies with improved specificity and reduced toxicity.

6. Conclusion

The computational investigation successfully identified novel AKT inhibitors with key pharmacophore features from the ZINC natural compound library. The validated pharmacophore model demonstrated strong

predictive reliability and was applied to screen the ZINC database, followed by molecular docking against the AKT protein (PDB ID: 8Q61). Among the screened compounds, ZINC 32109687 achieved the highest docking score; however, its predicted carcinogenicity, immunotoxicity, and mutagenicity limited its suitability as a lead. In contrast, ZINC 20412215 was selected as the most promising candidate due to its favourable pharmacokinetic properties, including high gastrointestinal absorption, desirable ADME profile, and absence of major toxicity risks, along with strong binding affinity to AKT.

Further, the study provides detailed information on these computational findings in the development. Future work will focus on experimental validation through *in vitro* kinase inhibition assays, structural optimization of the lead scaffold to further enhance activity and safety, and molecular dynamics simulations to confirm binding stability and interaction persistence. These steps can potentiate in advancing ZINC 20412215 as a lead therapeutic scaffold for targeting the mTOR/AKT pathway in breast cancer.

7. Acknowledgments

We extend our gratitude to the Management of SRM College of Pharmacy and SRM Institute of Science and Technology for their unwavering support and encouragement. We also thank the editorial and reviewing team of the journal for their valuable contributions.

8. Author Contribution

Sanjana and Sathiya Priya: Data curation, methodology, writing-original draft; Varshini and Devakeerthana: Data curation and writing-original draft; Venkatesan and Anjana: Reviewing and editing; Bharath Kumar: Supervision, resources and writing review. All authors have read and agreed to the published version of the manuscript.

9. References

1. Roshandel G, Ferlay J, Semnani S, Fazel A, Naeimi-Tabiei M, Ashaari M, *et al.* Recent cancer incidence trends and short-term predictions in Golestan, Iran 2004-2025. Cancer Epidemiol. 2020; 67:101728. PMid: 32554298. https://doi.org/10.1016/j.canep.2020.101728
2. Filho AM, Laversanne M, Ferlay J, Colombet M, Pineros M, Znaor A, *et al.* The GLOBOCAN 2022 cancer estimates: Data sources, methods, and a snapshot of the cancer burden worldwide. Int J Cancer. 2025; 156(7):1336-1346. PMid: 39688499. https://doi.org/10.1002/ijc.35278
3. Sung H, Ferlay J, Siegel RL, Laversanne M, Soerjomataram I, Jemal A, Bray F. Global cancer statistics 2020: GLOBOCAN estimates of incidence and mortality worldwide for 36 cancers in 185 countries. CA Cancer J Clin. 2021; 71(3):209-249. PMid: 33538338. https://doi.org/10.3322/caac.21660
4. Arnold M, Morgan E, Rumgay H, Mafra A, Singh D, Laversanne M, Vignat J, *et al.* Current and future burden of breast cancer: Global statistics for 2020 and 2040. Breast. 2022; 66:15-23. PMid: 36084384. PMCid: PMC9465273. https://doi.org/10.1016/j.breast.2022.08.010
5. Islami F, Ward EM, Sung H, Cronin KA, Tangka FKL, Sherman RL, *et al.* Annual report to the nation on the status of cancer, Part 1: National cancer statistics. J Natl Cancer Inst. 2021; 113(12):1648-1669. PMid: 34240195. PMCid: PMC8634503. https://doi.org/10.1093/jnci/djab131
6. Asghar MS, Yasmin F, Babar MS, Bin Zafar MD, Ismail Shah SM, Tahir MJ. Clinical characteristics and outcomes of cancer patients and their hospital course during the COVID-19 pandemic in a developing country. Ann Med Surg. 2022; 74:103284. PMid: 35127069. PMCid: PMC8800933. https://doi.org/10.1016/j.amsu.2022.103284
7. Rahman MM, Islam MR, Akash S, Harun-Or-Rashid M, Ray TK, Rahaman MS, *et al.* Recent advancements of nanoparticles application in cancer and neurodegenerative disorders: At a glance. Biomed Pharmacother. 2022; 153:113305. PMid: 35717779. https://doi.org/10.1016/j.biopha.2022.113305
8. Zhang J, Wu Y, Li Y, Li S, Liu J, Yang X, Xia G, Wang G. Natural products and derivatives for breast cancer treatment: From drug discovery to molecular mechanism. Phytomedicine. 2024; 129:155600. PMid: 38614043. https://doi.org/10.1016/j.phymed.2024.155600
9. Nayak SR, Haridevamuthu B, Murugan R, Dhivya LS, *et al.* Furan-based chalcone protects β-cell damage and improves glucose uptake in alloxan-induced zebrafish diabetic model *via* influencing Peroxisome Proliferator-Activated Receptor agonists (PPAR-γ) signaling. Process Biochem. 2024; 142:149-161. https://doi.org/10.1016/j.procbio.2024.04.012
10. Cragg GM, Pezzuto JM. Natural products as a vital source for the discovery of cancer chemotherapeutic and chemopreventive agents. Med Princ Pract. 2016; 25(Suppl 2):41-59. PMid: 26679767. PMCid: PMC5588531. https://doi.org/10.1159/000443404
11. Rayan A, Raiyn J, Falah M. Nature is the best source of anticancer drugs: Indexing natural products for their

anticancer bioactivity. Plos One. 2017; 12(11):e0187925. PMid: 29121120. PMCid: PMC5679595. https://doi.org/10.1371/journal.pone.0187925

12. Gupta AP, Pandotra P, Kushwaha M, Khan S, Sharma R, Gupta S. Alkaloids: A source of anticancer agents from nature. Stud Nat Prod Chem. 2015; 46:341-445. https://doi.org/10.1016/B978-0-444-63462-7.00009-9
13. Fridlender M, Kapulnik Y, Koltai H. Plant derived substances with anti-cancer activity: From folklore to practice. Front Plant Sci. 2015; 6:799. PMid: 26483815. PMCid: PMC4589652. https://doi.org/10.3389/fpls.2015.00799
14. Huang M, Lu JJ, Ding J. Natural products in cancer therapy: Past, present and future. Nat Prod Bioprospect. 2021; 11(1):5-13. PMid: 33389713. PMCid: PMC7933288. https://doi.org/10.1007/s13659-020-00293-7
15. Butti R, Das S, Gunasekaran VP, Yadav AS, Kumar D, Kundu GC. Receptor tyrosine kinases (RTKs) in breast cancer: Signaling, therapeutic implications and challenges. Mol Cancer. 2018; 17(1):34. PMid: 29455658. PMCid: PMC5817867. https://doi.org/10.1186/s12943-018-0797-x
16. Paplomata E, O'Regan R. The PI3K/AKT/mTOR pathway in breast cancer: Targets, trials and biomarkers. Ther Adv Med Oncol. 2014; 6(4):154-166. PMid: 25057302. PMCid: PMC4107712. https://doi.org/10.1177/1758834014530023
17. Cragg GM, Grothaus PG, Newman DJ. Impact of natural products on developing new anti-cancer agents. Chem Rev. 2009; 109(7):3012-3043. PMid: 19422222. https://doi.org/10.1021/cr900019j
18. Chu N, Viennet T, Bae H, Salguero A, Boeszoermenyi A, Arthanari H, Cole PA. The structural determinants of PH domain-mediated regulation of Akt revealed by segmental labeling. Elife. 2020; 9:e59151. PMid: 32744507. PMCid: PMC7438110. https://doi.org/10.7554/eLife.59151
19. Liu P, Wang Z, Wei W. Phosphorylation of Akt at the C-terminal tail triggers Akt activation. Cell Cycle. 2014; 13(14):2162-2164. PMid: 24933731. PMCid: PMC4111671. https://doi.org/10.4161/cc.29584
20. Liu P, Begley M, Michowski W, Inuzuka H, Ginzberg M, *et al*. Cell-cycle-regulated activation of Akt kinase by phosphorylation at its carboxyl terminus. Nature. 2014; 508(7497):541-545. PMid: 24670654. PMCid: PMC4076493. https://doi.org/10.1038/nature13079
21. Fruman DA, Rommel C. PI3K and cancer: Lessons, challenges and opportunities. Nat Rev Drug Discov. 2014; 13(2):140-156. PMid: 24481312. PMCid: PMC3994981. https://doi.org/10.1038/nrd4204
22. Xing Y, Lin NU, Maurer MA, Chen H, Mahvash A, Sahin A, Akcakanat A, *et al*. Phase II trial of AKT inhibitor MK-2206 in patients with advanced breast cancer who have tumors with PIK3CA or AKT mutations, and/or PTEN loss/PTEN mutation. BGR. 2019; 21:1-2. PMid: 31277699. PMCid: PMC6612080. https://doi.org/10.1186/s13058-019-1154-8
23. Sangai T, Akcakanat A, Chen H, Tarco E, Wu Y, Do KA, *et al*. Biomarkers of response to Akt inhibitor MK-2206 in breast cancer. Clin Cancer Res. 2012; 18(20):5816-5828. PMid: 22932669. PMCid: PMC3772348. https://doi.org/10.1158/1078-0432.CCR-12-1141
24. Yan C, Yang J, Saleh N, Chen SC, Ayers GD, Abramson VG, Mayer IA, Richmond A. Inhibition of the PI3K/mTOR pathway in breast cancer to enhance response to immune checkpoint inhibitors in breast cancer. Int J Mol Sci. 2021; 22(10):5207. PMid: 34069042. PMCid: PMC8156389. https://doi.org/10.3390/ijms22105207
25. Hameed R, Khan A, Khan S, Perveen S. Computational approaches towards kinases as attractive targets for anticancer drug discovery and development. Anticancer Agents Med Chem. 2019; 19(5):592-598. PMid: 30306880. https://doi.org/10.2174/1871520618666181009163014
26. Chandra Mouli HM, Vinod A, Kumari S, Tiwari AK, Kathiravan MK, *et al*. Deuterated driven new chemical entities: An optimistic way to improve therapeutic efficacy. Bioorg Chem. 2023; 135:106490. PMid: 37001472. https://doi.org/10.1016/j.bioorg.2023.106490
27. Chitre TS, Kathiravan MK, Bothara KG, Bhandari SV, Jalnapurkar RR. Pharmacophore optimization and design of competitive inhibitors of thymidine monophosphate kinase through molecular modeling studies. Chemical Biology Drug Design. 2011; 78(5):826-834. PMid: 21801308. https://doi.org/10.1111/j.1747-0285.2011.01200.x
28. Laamari Y, Bimoussa A, Mourad F, Chagaleti BK, Saravanan V, *et al*. Multitargeted molecular docking and dynamics simulation of thymol-based chalcones against cancer protein markers: Synthesis, characterisation, and computational study. J Mole Struct. 2024; 1317:139116. https://doi.org/10.1016/j.molstruc.2024.139116
29. Kathiravan MK, Shishoo CJ, Kumar KG, Roy SK, Mahadik KR, Kadam SS, Jain KS. Synthesis and antihyperlipidemic activity of some novel condensed 2-chloroalkyl-4-chloro/hydroxy-5, 6-disubstituted pyrimidines. Arzneimittel-Forschung. 2007; 57(09):599-606. PMid: 17966759. https://doi.org/10.1055/s-0031-1296655
30. Mouli HC, Vinod A, Kumari S, Tiwari AK, Kathiravan MK, Ravichandiran V, Peraman R. Deuterated driven new chemical entities: An optimistic way to improve therapeutic efficacy. Bioorg Chem. 2023; 135:106490. PMid: 37001472. https://doi.org/10.1016/j.bioorg.2023.106490
31. Chagaleti BK, Kumar SB, Rajagopal R, Alfarhan A, Arockiaraj J, *et al*. Targeting cyclin-dependent kinase 2 CDK2: Insights from molecular docking and dynamics simulation - A systematic computational approach to discover novel cancer therapeutics. Comput Biol Chem. 2024; 112:108134. PMid: 38964206. https://doi.org/10.1016/j.compbiolchem.2024.108134

32. Varela C, Silva F, Costa G, Cabral C. Alkaloids: Their relevance in cancer treatment. New Insights Into Glioblastoma. Elsevier. 2023: pp. 361-401. https://doi.org/10.1016/B978-0-323-99873-4.00006-2
33. El Khalki L, Maire V, Dubois T, Zyad A. Berberine impairs the survival of triple negative breast cancer cells: Cellular and molecular analyses. Molecules. 2020; 25(3):506. PMid: 31991634. PMCid: PMC7036777. https://doi.org/10.3390/molecules25030506
34. Sun Y, Gu Y, Gao X, Jin X, Wink M, Sharopov FS, Yang L, Sethi G. Lycorine suppresses the malignancy of breast carcinoma by modulating epithelial mesenchymal transition and β-catenin signaling. Pharmacol Res. 2023; 195:106866. PMid: 37499704. https://doi.org/10.1016/j.phrs.2023.106866
35. Packiapalavesam SD, Saravanan V, Mahajan AA, Almutairi MH, *et al*. Identification of novel CA IX inhibitor: Pharmacophore modeling, docking, DFT, and dynamic simulation. Comput Biol Chem. 2024; 110:108073. PMid: 38678727. https://doi.org/10.1016/j.compbiolchem.2024.108073
36. Chagaleti BK, Saravanan V, Vellapandian C, Kathiravan MK. Exploring cyclin-dependent kinase inhibitors: A comprehensive study in search of CDK-6 inhibitors using a pharmacophore modelling and dynamics approach. RSC Adv. 2023; 13(48):33770-33785. PMid: 38019988. PMCid: PMC10655667. https://doi.org/10.1039/D3RA05672D
37. Irrou E, AitElmachkouri Y, El Haddad S, Chagaleti BK, Mague JT, *et al*. Synthesis of novel N4-substituted and C2-disubstituted 1, 4-benzothiazine-1, 1-dioxide derivatives: Integrative computational strategies for breast cancer therapy. J Mol Struct. 2025; 1338:142310. https://doi.org/10.1016/j.molstruc.2025.142310
38. Chagaleti BK, Saravanan V, Kathiravan MK. Discovery of novel CDK2 inhibitors for cancer treatment: integrating ligand-based pharmacophore modelling, molecular docking, DFT, ADMET, and molecular dynamics simulation studies. Beni-Suef Univ J Basic and Appl Sci. Springer. 2024; 13(1):118. https://doi.org/10.1186/s43088-024-00577-8
39. Lipinski CA, Lombardo F, Dominy BW, Feeney PJ. Experimental and computational approaches to estimate solubility and permeability in drug discovery and development settings. Adv Drug Deliv Rev. 1997; 23(1-3):3-25. https://doi.org/10.1016/S0169-409X(96)00423-1
40. Gopinath P, Kathiravan MK. Docking studies and molecular dynamics simulation of triazole benzene sulfonamide derivatives with human carbonic anhydrase IX inhibition activity. RSC Adv. 2021; 11(60):38079-38093. PMid: 35498092. PMCid: PMC9044052. https://doi.org/10.1039/D1RA07377J
41. Irrou E, Ait Elmachkouri Y, El Haddad S, Chagaleti BK, Mague JT, *et al*. Synthesis of novel N4-substituted and C2-disubstituted 1, 4-benzothiazine-1, 1-dioxide derivatives: Integrative computational strategies for breast cancer therapy. J Mole Struct. 2025; 1338:142310. https://doi.org/10.1016/j.molstruc.2025.142310
42. A. Daina, O. Michielin, V. Zoete, SwissADME: A free web tool to evaluate pharmacokinetics, drug-likeness and medicinal chemistry friendliness of small molecules. Sci Rep. 2017; 7:1-13. PMid: 28256516. PMCid: PMC5335600. https://doi.org/10.1038/srep42717
43. Banerjee P, Eckert AO, Schrey AK, Preissner R. ProTox-II: A webserver for the prediction of toxicity of chemicals. Nucleic Acids Res. 2018; 46(W1):W257-W263. PMid: 29718510. PMCid: PMC6031011. https://doi.org/10.1093/nar/gky318
44. Haridevamuthu B, Nayak SR, Madesh S, Dhivya LS, Chagaleti BK, *et al*. A novel brominated chalcone derivative as a promising multi-target inhibitor against multidrug-resistant *Listeria monocytogenes*. Microb Pathog. 2024; 196:106968. PMid: 39307201. https://doi.org/10.1016/j.micpath.2024.106968
45. Jena A, Prakashraj C, Chagaleti BK, Kathiravan MK, Kumar BS. *In silico* design and synthesis of some new imidazole derivatives for tuberculosis. Indian J Heterocycl Chem. 2023; 33(1):43-49. https://doi.org/10.59467/IJHC.2023.33.43
46. Jain KS, Bariwal JB, Kathiravan MK, Raskar VK, Wankhede GS, Londhe NA, *et al*. An efficient and rapid synthesis of 2-amino-4-arylthiazoles employing microwave irradiation in water. Green Sustain Chem. 2011; 1(2):35-38. https://doi.org/10.4236/gsc.2011.12007
47. Salake AB, Chothe AS, Nilewar SS, Khilare M, Meshram RS, Pandey AA, Kathiravan MK. Design, synthesis, and evaluations of antifungal activity of novel phenyl (2H-tetrazol-5-yl) methanamine derivatives. J Chem Biol. 2013; 7(1):29-35. PMid: 24432136. PMCid: PMC3877410. https://doi.org/10.1007/s12154-013-0103-8